

Growth of equilibrium polymers under non-equilibrium conditions

Francesco Sciortino¹, Cristiano De Michele¹ and Jack F Douglas²

¹ Dipartimento di Fisica and INFM-CNR-SOFT, Università di Roma La Sapienza, Piazzale Aldo Moro 2, 00185 Roma, Italy

² Polymers Division, National Institute of Standards and Technology, Gaithersburg, MD 20899, USA

Received 28 November 2007, in final form 4 February 2008

Published 4 March 2008

Online at stacks.iop.org/JPhysCM/20/155101

Abstract

We investigate the kinetics of self-assembly by means of Brownian dynamics simulation based on a idealized fluid model (two ‘sticky’ spots on a sphere) in which the particles are known to form into dynamic polymer chains at equilibrium. To illustrate the slow evolution of the properties of these self-assembling fluids to their equilibrium assembled state values at long times, we perform Brownian dynamics simulations over a range of quench depths from the high temperature unassembled state to the low temperature assembled state. We investigate the time dependence of the average chain length (cluster mass), the order parameter for the assembly transition (fraction of particles in the chain state) and the potential energy of the fluid. The rate constant governing the self-assembly ordering process depends both on kinetic-related factors (the particle hydrodynamic radius and the fluid viscosity) and on thermodynamic energetic variables governing the self-assembly transition (i.e., the entropy and enthalpy of assembly). We provide evidence that an essentially parameter-free description of the polymerization kinetics can be formulated for this model.

(Some figures in this article are in colour only in the electronic version)

1. Introduction

There is growing interest in exploiting self-assembly to create functional nanostructures for material and biological science applications [1–27]. Recently, there have been numerous experimental studies [1–5, 14, 28–30] aimed at creating model self-assembling systems, simulations that search for essential physical features governing the form of self-assembly and the dynamics of the assembly process [6–13, 31–35] and there are ongoing efforts to develop improved analytic theories of self-assembly that can provide a meaningful guide to experimental and simulation investigations in this area [36–41].

Although there have been many studies of self-assembly, our understanding of this phenomenon remains rudimentary in comparison to thermodynamic transitions such as liquid phase separation and crystallization. Particular progress has been made in developing predictive molecular theories of equilibrium polymerization (equilibrium self-assembly of polymer chains) in the absence of solvent (or equivalently in solution of associating species where solvent is treated as a continuum) based on Wertheim theory [42–44] and the predictions of the equilibrium properties of this class of

associating fluids has been strikingly confirmed by Monte Carlo simulation [45]. The problem can be formulated equivalently in terms of association–dissociation equilibria and lattice model computations based on this framework have also been validated for both chain assembly and phase separation in the Stockmayer fluid [46]. Fundamental progress has also been made based on the Wertheim theory [42–44] for particles exhibiting multifunctional (patchy) interactions which are necessary for describing branched equilibrium polymers and the thermally reversible gelation in multifunctional associating fluids. Wertheim theory has also provided insights into the phase separation that occurs in these multifunctional fluids, even in the absence of isotropic van der Waals interactions [41, 47].

Despite the progress, the models are idealized and there is the need for more theoretical development for even these simplest models of self-assembly. The molecular interaction models of self-assembly do not yet include many effects that are prevalent in real fluids exhibiting equilibrium polymerization, such as ring formation in unbranched chains, loop formation in branched polymer structures, activation

and inhibition of polymerization by chemical initiators and inhibitors, thermal activation of polymerization and photoactivation of polymerizing species. These constraints can have a large impact on the thermodynamics properties of polymers exhibiting equilibrium polymerization [36–39].

We also note that the recent advances in modeling the equilibrium polymerization of linear and branched polymers in freely-associating [37] particle systems (unconstrained by the factors just mentioned) involve only the equilibrium properties of these fluids and that rather little is firmly established about the dynamics of even these simple associating fluids. The present work directly addresses this problem and thereby focuses directly on developing a molecular understanding of the self-assembly of linear equilibrium polymer chains as a direct extension of our previous work describing the basic equilibrium properties of these model fluids.

There are notable previous efforts at modeling the dynamics of chain self-assembly. Based on early analytic work by Cates and co-workers [48, 49] on modeling equilibrium chain polymerization using statistical arguments, Milchev and Rouault [50–52] performed lattice bond-fluctuation Monte Carlo simulations of equilibrium polymerization where both equilibrium and dynamical properties were considered. These works provide insights into the role of excluded volume interactions in the self-assembly process and a check on the scaling arguments by Cates and co-workers to describe the effects of these interactions on polymerization properties. Milchev and Rouault [50–52] also made pioneering numerical studies of the growth of the average chain length following a stepwise change in thermodynamic conditions to check the mean field dynamical theory of Cates and co-workers [49]. These simulations confirmed the main features of Cates theory. Simulations were formulated in terms of Monte Carlo move rules for particle displacements and particle bonding and breaking so that the rate parameters of these simulations are not fully expressed in terms of molecular parameters. In more recent work, Ryckaert *et al* [53] followed up on Milchev’s simulations using off-lattice Brownian dynamics and confirmed the same pattern of behavior found in the lattice model calculations. These simulations also involved adjustable rate parameters for the bonding–dissociation process. While these former studies of the dynamics of self-assembly provide much information about the thermodynamics and dynamics of polymer self-assembly, they do not provide a predictive molecular model framework and the direct validation of the molecular model by simulation that we seek. We are concerned with making predictions, without any free molecular parameters, of the dynamic properties of equilibrium polymers since we anticipate that such a description will provide a deeper understanding of the self-assembly more broadly.

The study of the dynamics of even the simplest self-assembling systems entails a number of distinct dynamical effects that need to be understood in order to exert effective control over the self-assembly process. First, there is the basic issue of characterizing the rate at which self-assembling systems form or disintegrate by jumping the thermodynamic conditions from thermodynamic conditions governing the disordered (unassembled) and ordered (assembled) states, and

vice versa, respectively. Self-assembly does not normally conform to a first or second order phase transition, but clearly this transformation corresponds to a type of thermodynamic transition in the broad sense. What is the kinetics of this ordering process? The next level of questions concerns the description of stress, dielectric and other relaxation processes in these dynamically heterogeneous fluids. These questions are clearly basic to understanding static and dynamic properties of associating fluids. We anticipate that ideas that have been developed in the dynamic critical phenomena of complex fluids, such as the mode coupling theory of critical dynamics, can be usefully adapted to this problem when large scale structures are formed in the assembly process. Finally, at an even higher complexity level, equilibrium polymers such as actin and synthetic equilibrium polymers [54] can exhibit wavefronts of self-assembly under non-equilibrium conditions that are similar in character to the formation of crystallization fronts in the sense that these waves develop progressively with a constant velocity as a locally ordered region grows into an unstable surroundings. The theoretical description of this phenomenon, which underlies many biological processes such as cell movement through actin polymerization, in terms of molecular parameters clearly offers many challenges for future research.

In the present work, we focus on the most basic problem of this kind, characterization of the dynamics of self-assembly under uniform thermodynamic conditions that are assumed to exist following a temperature jump. In section 2, we briefly describe our minimal molecular model of fluid which exhibits reversible equilibrium polymerization upon cooling. This model, which is the same as described by us in a previous work focusing on the equilibrium properties of equilibrium polymerization [45], basically involves hard spheres with two sticky spots at their poles that cause the particles to chain at low temperatures. Since we are interested in describing the dynamics of these fluids here, we introduce Brownian dynamics description of the fluid dynamics in section 3. This modeling does not include intermolecular and intramolecular hydrodynamics, so the chain dynamics in our fluid corresponds to idealized Rouse chain dynamics. However, the modeling does include self-friction effects associated with the chain beads so that the dynamics depends on the fluid viscosity through the bead friction coefficient (or equivalently through the bare monomer diffusion coefficient). We then develop a mean field Smoluchowski kinetic model of the chain assembly dynamics in section 4 and validate molecular models of binary particle association and dissociation rate constants in this section. This combination of rate constants allows us to then make predictions of the kinetics of the assembly process based on our kinetic assembly model. We first consider the analytic predictions for the evolution of the chain length distribution following a temperature jump and the growth of the average chain length $\bar{l}(t)$ in time t from the disordered to the fully assembled state at equilibrium. We also consider the evolution of the potential energy per particle E at equilibrium, especially since this quantity provides a good measure of the approach of the fluid to equilibrium in simulation studies. Finally, we consider perhaps the most basic property of self-assembling

systems from an experimental viewpoint, the time dependence of the order parameter $\Phi(t)$ for the self-assembly transition, which is defined as the fraction of particles in the assembled particle (polymeric) state at time t . In the experimental literature $\Phi(t)$ is normally termed as a progress curve since this quantity, relative to its long time equilibrium value $\Phi(t \rightarrow \infty) \equiv \Phi^*$, describes the progressive development of the self-assembly process [13, 55–57]. Experimentally, $\Phi(t)$ is normally measured by spectroscopic means. We find that rate constant governing the growth of $\Phi(t)$ in fluids undergoing equilibrium polymerization, following a homogeneous temperature quench, depends on both the solvent viscosity through the friction coefficient of the polymer beads, and the thermodynamic variables related to the depth of the temperature quench (enthalpy and entropy of assembly), which are fully specified in our terms of our molecular model parameters.

2. The two-patchy sites model

The studied model for bifunctional monomers is the same introduced in [45]. Each monomer is modeled as an hard-sphere (HS) particles (of diameter σ , the unit of length) whose surface is decorated by $M = 2$ identical sites oppositely located. Sites on different particles interact via a square-well potential (of depth $-u_0$ and well-width δ), so that the resulting interaction $V(\mathbf{1}, \mathbf{2})$ between particles $\mathbf{1}$ and $\mathbf{2}$ is,

$$V(\mathbf{1}, \mathbf{2}) = V_{\text{HS}}(\mathbf{r}_{12}) + \sum_{i=1,2} \sum_{j=1,2} V_W(\mathbf{r}_{12}^{ij}) \quad (1)$$

where V_{HS} is the hard-sphere potential, $V_W(x)$ is a square-well interaction and \mathbf{r}_{12} and \mathbf{r}_{12}^{ij} are respectively the vectors joining the particle–particle centers and the site–site (on different particles) locations. Temperature is measured in units of the potential depth (i.e. Boltzmann constant $k_B = 1$). The choice of well-width $\delta = 0.5(\sqrt{5} - 2\sqrt{3} - 1)\sigma \approx 0.119\sigma$ guarantees that each site is engaged at most in one bond. Hence, each particle can form only up to two bonds and, correspondingly, the lowest energy per particle (‘sticking energy’) is simply the bead contact value of the potential, $-u_0$.

3. Brownian dynamics simulations

We have performed Brownian dynamics simulations (using the algorithm described in the appendix) for a system of $N = 10^4$ particles in a volume V . The Brownian dynamic code—which neglects hydrodynamic interactions—requires as input, beside the temperature, the diffusion coefficient of the monomer D_1 , or equivalently the viscosity of the solvent η . The relation between D_1 and η is given by $D_1 = \frac{k_B T}{3\pi\sigma\eta}$. In this paper we will report time in scaled units $\hat{t} = t/t_o$ with $t_o = \sigma^2/6D_1$, so that $\hat{t} = 1$ indicates the time it takes an isolated monomer to diffuse over a distance equal to the particle size. All quantities with an $\hat{}$ refer to scaled time units. A conversion to physical time requires the actual temperature and the solvent viscosity, according to $t = \frac{\pi\sigma^3\eta}{2k_B T} \hat{t}$.

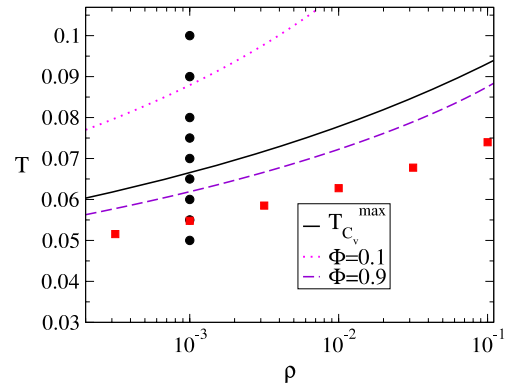


Figure 1. Phase diagram of the studied model. Curves indicate characteristic transition lines for self-assembly, as indicated in the inset. These lines include the ‘polymerization transition line’ where C_v has a maximum, the self-assembly ‘onset line’ ($\Phi = 0.1$) where appreciable polymerization first initiates, and the ‘saturation curve’ ($\Phi = 0.9$) where the self-assembly transition is essentially ‘finished’ [36, 61]. Filled circles indicate thermodynamic states investigated by simulation along a constant $\rho = 0.001$ path (circles) and along a constant $\bar{l} = 8$ path (squares).

We have studied the equilibration process after a temperature jump from the high temperature unassembled state to the low temperature assembled state. Two sets of simulations were performed. The first set is composed by a sequence of different state points (T, ρ) , such that the equilibrium final state is characterized by an identical average polymerization length $\bar{l} = 8$. The second set is composed by the same monomer number density $\rho = 10^{-3}$, but different temperatures. Figure 1 shows the relative location of all studied state points in the $(\rho-T)$ phase diagram of the model (from [45]). In the case of equilibrium polymers, the relevant lines are provided by the location of the specific heat maximum C_v^{max} (along which the fluctuations in the number of bonds are maxima) and by lines of iso-extent of polymerization Φ . Such a quantity, which measures the fraction of material in polymeric state, plays the role of the order parameter of the polymerization transition [36, 37, 58–60]. The studied points cross the polymerization transition line. We also note that, due to computational requirements, all studied points are characterized by average chain lengths smaller or comparable to the persistence length of the present model. Entanglement effects are not relevant to the present study.

As a result of the large system size studied, average quantities are affected by less than 3% relative error. Chain length distributions $N_l(t)$, whose signal covers up to six orders of magnitude are affected by an error proportional to $1/\sqrt{lN_l(t)}$, which progressively increases on decreasing l .

4. Equilibration

A possible modeling of the equilibration process is provided by the Smoluchowski equation [62], specialized to the case of linear chains of independent bonds [49, 63]. The equation provides the time evolution of the chain length distribution $N_l(t)$ (number of chains of length l observed at time t), in the chemical limit [64], i.e. provided that the rate constant for

bonding k_{bonding} and breaking k_{breaking} are independent on the chain length. In the chemical limit, the diffusive part of the rate constant (which could be a function of the chain length), is negligible as compared to the bonding part, which is indeed l independent [64]. The evolution of N_l is given by

$$\frac{dN_l}{dt} = -k_{\text{breaking}}(l-1)N_l + 2k_{\text{breaking}} \sum_{j=l+1}^{\infty} N_j + \frac{1}{2} \frac{k_{\text{bonding}}}{V} \sum_{j=1}^{l-1} N_j N_{l-j} - N_l \frac{k_{\text{bonding}}}{V} \sum_{j=1}^{\infty} N_j. \quad (2)$$

The four contributions to $\frac{dN_l}{dt}$ can be respectively identified with the breaking of a cluster of size N_l , the breaking of a cluster of size larger than l in two pieces, one of which has length l , the joining of two clusters to form a chain of length l and the joining of a cluster of size l with a different chain. Equation (2) assumes that the bonding and breaking rates are independent on the cluster size (note that k_{breaking} has the dimension of inverse of time, while k_{bonding} is a volume divided by time). The two rate constant k_{bonding} and k_{breaking} are not independent, since they must guarantee that the equilibrium distribution arises from the long time limit solution of the equation.

4.1. Binary particle association constant

The study of the aggregation dynamics at short times provides a method to evaluate unambiguously k_{bonding} . Indeed, starting from an unassembled state, only monomers are present at time $t = 0$ and hence $N_i(t = 0) = N\delta_{i,1}$. At short times, equation (2) simplifies to the simple equations involving the bonding rate,

$$\frac{dN_1}{dt} = -\frac{k_{\text{bonding}}}{V} N_1 N_1 \quad (3)$$

$$\frac{dN_2}{dt} = \frac{1}{2} \frac{k_{\text{bonding}}}{V} N_1 N_1 = -\frac{1}{2} \frac{dN_1}{dt}. \quad (4)$$

The potential energy E of the system measures the number of bonds. At short times, the number of bonds is identical to the number of dimers. Hence $E = -u_0 N_2$ and (since $N_1 \approx N$ at short time)

$$\frac{d\left(\frac{E}{Nu_0}\right)}{dt} = -\frac{1}{2} k_{\text{bonding}} \rho \quad (5)$$

which, at short time gives

$$\frac{E(t)}{Nu_0} = -\frac{1}{2} k_{\text{bonding}} \rho t. \quad (6)$$

Hence, from a study of the initial behavior of the potential energy it is possible to extract the density and temperature dependence of the bonding rate k_{bonding} .

Figure 2(a) shows the time dependence of $\frac{2E(t)}{Nu_0\rho t}$ versus \hat{t} . As predicted by equation (6), the quantity $\frac{2E(t)}{Nu_0\rho t} = -k_{\text{bonding}}$ shows a constant plateau whose value provides an estimate for k_{bonding} . A similar behavior is observed also in the group of simulations at constant ρ , as shown in figure 2(b). Both set of data are consistent with a value of $\hat{k}_{\text{bonding}} \approx 0.06 \pm 0.02$, independent on T and ρ .

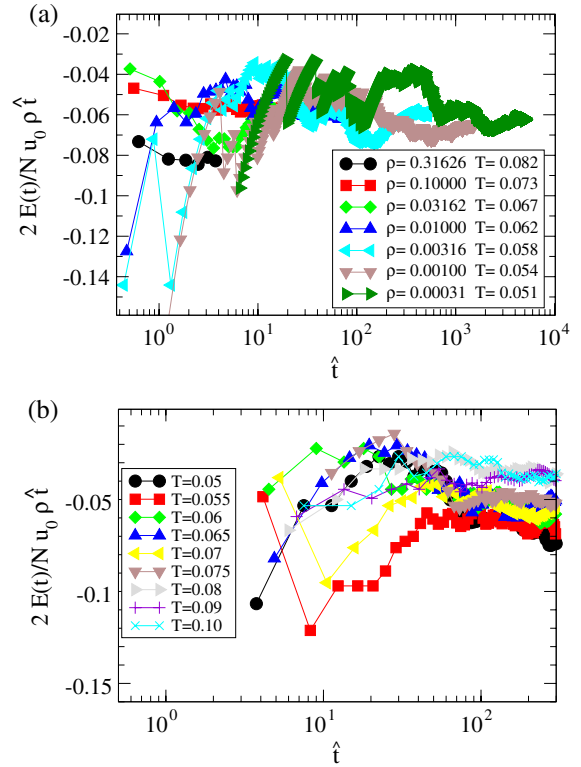


Figure 2. Behavior of the potential energy at short time: data are reported following equation (6), so that the value of k_{bonding} can be read by the graph. In (a), the simulations refer to different ρ and T values, such that the final equilibrium state is characterized by $\bar{l} = 8$. In (b) the simulations refer to different T values, but at $\rho = 0.001$. Note that data refer to the time interval in which the energy per particle goes from zero to $-0.05u_0$. The zig-zag short time behavior is an artifact of the discrete bonding normalized by a continuous variable (time).

We note that the Smoluchowski Brownian dimer formation rate constant is $k_{\text{bonding}}^{\text{Brownian}} = \frac{8kT}{3\eta}$ [62]. Since $D_1 = \frac{kT}{3\pi\sigma\eta}$, measuring time in the same scaled unit as above gives $\hat{k}_{\text{bonding}}^{\text{Brownian}} = \frac{8\pi\sigma^3}{6} \approx 4.19$. The bonding constant for the patch model we have used is thus about 70 time smaller than the one of the corresponding spherical model, a figure consistent with expectations based on the general expression for Brownian association rates in the presence of orientational constraints [65].

4.2. Binary particle dissociation constant

The study of the full evolution of the system following a T -jump provides a method for estimating k_{breaking} . It also allows for a test of the theoretical description.

In equilibrium (i.e. $dN_l/dt = 0$), the chain length distribution N_l (number of chains of length l) is given by,

$$N_l = \frac{N}{\bar{l}^2} \left(1 - \frac{1}{\bar{l}}\right)^{l-1} \quad (7)$$

normalized in such a way that

$$\sum_{l=1}^{\infty} l N_l = N \quad (8)$$

where \bar{l} indicates the ρ and T dependent equilibrium average chain length.

Substituting the known N_l equilibrium distribution in equation (2), one finds

$$\frac{k_{\text{bonding}}}{2k_{\text{breaking}}} = \frac{\bar{l}(\bar{l} - 1)}{\rho}. \quad (9)$$

The T and ρ dependence of \bar{l} is very well predicted by the Wertheim theory (see equation 11 of [45]). Substituting the predicted value for \bar{l} , gives

$$\frac{k_{\text{bonding}}\rho}{2k_{\text{breaking}}} = \exp\{-\beta(\Delta U_b - T\Delta S_b)\} \quad (10)$$

where ΔU_b and ΔS_b are the energy and entropy change in the bond process. The Wertheim theory provides precise expressions for ΔU_b and ΔS_b . Specifically, when $e^{\beta u_0} \gg 1$ (a very minor approximation since aggregation requires $T \ll u_0$ to be effective)

$$\Delta U_b = -u_0 \quad (11)$$

$$\Delta S_b/k_B = \ln \left[8\pi\rho \int_{\sigma}^{\sigma+\delta} g_{\text{HS}}(r)S(r)r^2 dr \right]. \quad (12)$$

where [45]

$$S(r) = \frac{(\delta + \sigma - r)^2(2\delta - \sigma + r)}{6\sigma^2 r} \quad (13)$$

is the fraction of solid angle available to bonding when two particles are located at relative center-to-center distance r and $g_{\text{HS}}(r)$ is the hard-sphere radial distribution function. At small densities, $g_{\text{HS}}(r) \approx 1$ and $V_b \equiv 4\pi \int_{\sigma}^{\sigma+\delta} S(r)r^2 dr = 0.000332$, so that

$$\Delta S_b/k_B = \ln [2\rho V_b] = \ln \left[2N \frac{V_b}{V} \right]. \quad (14)$$

Thus, the change in entropy is essentially provided by the logarithm of the ratio between the bonding volume V_b and the volume per site $V/2N$. Within the same approximations, the equilibrium relation between k_{bonding} and k_{breaking} becomes

$$k_{\text{breaking}} = \frac{k_{\text{bonding}}}{4V_b e^{\beta u_0}}. \quad (15)$$

The existence of a relation between k_{bonding} , k_{breaking} and \bar{l} , can be exploited to find the scaling properties of the evolution of the cluster size distribution. Indeed, dividing equation (2) by k_{breaking} gives,

$$\begin{aligned} \frac{dN_l}{d(k_{\text{breaking}}t)} &= -(l-1)N_l + 2 \sum_{j=l+1}^{\infty} N_j \\ &+ \frac{\bar{l}(\bar{l}-1)}{N} \sum_{j=1}^{l-1} N_j N_{l-j} - 2N_l \frac{\bar{l}(\bar{l}-1)}{N} \sum_{j=1}^{\infty} N_j. \end{aligned} \quad (16)$$

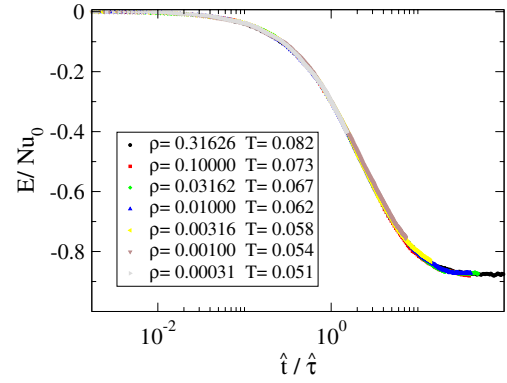


Figure 3. Reduced time representation of the evolution of the potential energy per particle. The reduced time \hat{t} has been chosen so that $E/N(\hat{t}) = -0.3 u_0$. Simulations refer to different ρ and T values, such that the final equilibrium state is characterized by $\bar{l} = 8$.

The evolution of the distribution function is thus only a function of the equilibrium final average length and of $k_{\text{breaking}}t$:

$$\frac{dN_l}{d(k_{\text{breaking}}t)} = f(\bar{l}, k_{\text{breaking}}t). \quad (17)$$

This suggests that all the equilibration curves for all cases in which the final equilibrium \bar{l} is identical should collapse on one single master curve and the scaling time $\tau \equiv \frac{1}{k_{\text{breaking}}}$ would provide an evaluation of the breaking constant. This is indeed what we find in figure 3.

5. Time dependence of \bar{l} , Φ and E

5.1. Evolution of the average length

The time dependence of the cluster size distribution can be obtained in a closed form solving equation (2), similarly to treatment by Cates and Candau for the continuous l case. Assuming that the chain length distribution retains the equilibrium shape, but with a t dependence average length $\bar{l}(t)$, i.e.,

$$N_l(t) = \frac{N}{\bar{l}(t)^2} \left(1 - \frac{1}{\bar{l}(t)} \right)^{l-1}, \quad (18)$$

after little algebra one finds

$$\frac{d\bar{l}(t)}{d(k_{\text{breaking}}t)} = \bar{l}(\bar{l} - 1) - \bar{l}(t)(\bar{l}(t) - 1) \quad (19)$$

which has the solution (for the case in which the polymerization increases upon time):

$$\begin{aligned} \bar{l}(t) &= \frac{1 + (2\bar{l} - 1) \tanh\left[\frac{k_{\text{breaking}}t}{2}(2\bar{l} - 1) + \phi\right]}{2} \\ \tanh[\phi] &= \frac{2\bar{l}(0) - 1}{2\bar{l} - 1}. \end{aligned} \quad (20)$$

Equation (20) implies that the growth rate for the equilibration dynamics is $[\frac{k_{\text{breaking}}}{2}(2\bar{l} - 1)]^{-1}$, which reduces to the Candau–Cates [49] expression for large \bar{l} values.

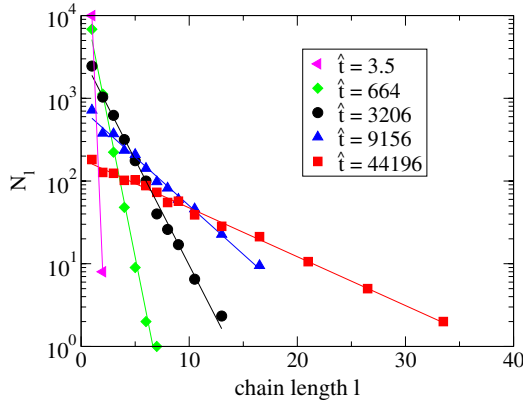


Figure 4. Evolution of the chain length distribution (symbols) at $T = 0.06275$ and $\rho = 0.01$ for different times. Lines are exponential lines to guide the eye. The distributions are calculated over one configuration of the system along its equilibration trajectory.

The solution in equation (20) describes quenches to state points characterized by an average chain length larger than the initial one. It is remarkable that the equilibration process predicted by the equation (2) predicts an evolution of the chain length distribution which maintains the equilibrium shape. Only the value of the average chain length changes with time. This property is not true for other types of equilibrium polymerization where the chains form and shrink from their ends [66].

A universal representation of the time dependence of $\bar{l}(t)$ is provided by a simple algebraic manipulation of equation (20), which can be written as

$$\frac{2\bar{l}(t) - 1}{2\bar{l} - 1} = \tanh \left[\frac{k_{\text{breaking}} t}{2} (2\bar{l} - 1) + \phi \right]. \quad (21)$$

An experimental study of the quantity $\frac{2\bar{l}(t) - 1}{2\bar{l} - 1}$ should reveal the typical tanh shape. For large \bar{l} , $\phi \rightarrow 0$ and $\frac{2\bar{l}(t) - 1}{2\bar{l} - 1} \approx l(t)/\bar{l}$ becomes an universal function of $k_{\text{breaking}} t \bar{l}$. It is also interesting to observe that, for deep quenches, using equation (10), (i.e., for large $\exp[\beta u_0]$), $k_{\text{breaking}} \approx k_{\text{bonding}} \rho \exp[\beta(\Delta U_b - T \Delta S_b)]/2$. Since k_{bonding} has no T or ρ dependence in it, the reduced time provides information of the bond free energy change.

Figure 4 shows the chain length distribution for several times after the T -quench. The distribution evolves continuously toward the equilibrium \bar{l} value retaining the exponential shape at all intermediate time. This suggests that the hypothesis behind equation (2) is satisfied.

Figure 5 shows the time evolution of the average length calculated from the simulation data with the theoretical predictions, using k_{breaking} as the only fitting parameter. The equilibrium value \bar{l} is indeed theoretically known from Wertheim theory and depends on the density and T of the system. Both sets of simulations are well described by equation (20).

We also note that, for very deep quenches, when breaking effects are negligible (or equivalently when $\bar{l} \gg 1$),

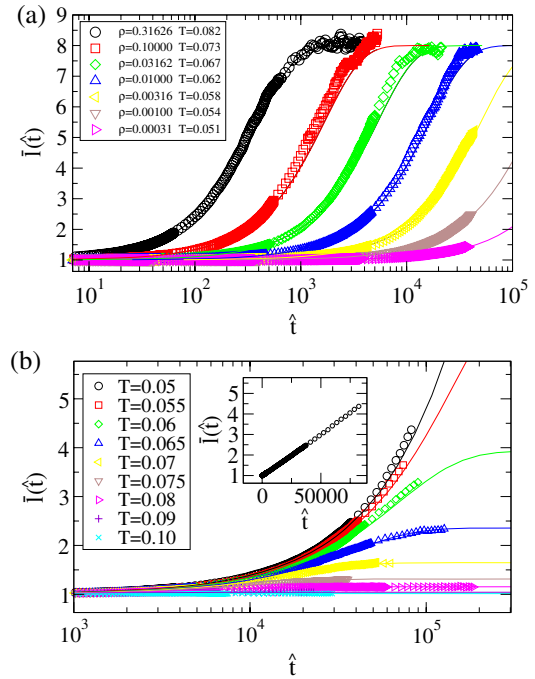


Figure 5. Evolution of the average chain length (symbols) and theoretical predictions (lines) for all studied simulations. In (a) simulations refer to different ρ and T values, such that the final equilibrium state is characterized by $\bar{l} = 8$. In (b) $\rho = 0.001$. The inset in (b) shows the linear growth law for the case $\rho = 0.001$ and $T = 0.05$.

equation (20) predicts as limiting behavior

$$\bar{l}(t) = 1 + \frac{k_{\text{bonding}} \rho t}{2}, \quad (22)$$

i.e. a linear growth of the chain length. This behavior is indeed observed in the deepest studied quench (inset of figure 5(b)).

In section 4.1 we have shown that in the present model $\hat{k}_{\text{bonding}} \approx 0.06$ (see figure 2). It is thus possible to predict k_{breaking} using equation (15) and compare the predictions with the results of the fitting. Such a comparison is reported in figure 6. The agreement is rather striking, considering the complete absence of any fitting parameter. From the value of k_{bonding} , a quantity which can easily be accessed experimentally or numerically from early stage measurements of the aggregation process, it is possible to predict rather precisely the entire time dependence of the equilibration process. This suggests that, as for the equilibrium properties, the reversible aggregation kinetics of bifunctional units can be described by a combination of the equilibrium Wertheim theory and bonding and breaking rate constants deduced from Smoluchowki theory.

5.2. Potential energy

The time dependence of the potential energy is related to the time dependence of the average length $\bar{l}(t)$. Indeed, as shown in [45], $-E(t)/Nu_0 = 1 - \bar{l}(t)^{-1}$. The comparison between the numerical data and the theory (with the same k_{breaking} values as in figure 5) is shown in figure 7. As for $\bar{l}(t)$, the time

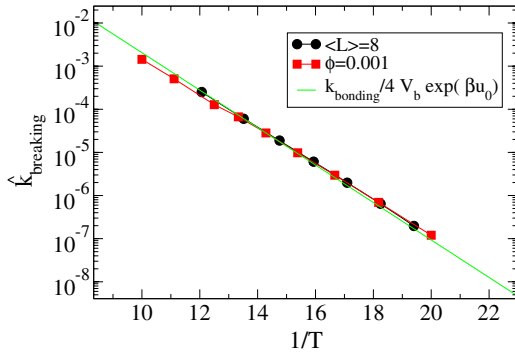


Figure 6. Temperature dependence of $\hat{k}_{\text{breaking}}$ as extracted from the fit of the time dependence of the potential energy to equation (20) and as predicted theoretically. Symbols refer (i) to simulations with different ρ and T values, such that the final equilibrium state is characterized by $\bar{l} = 8$ and (ii) to simulation at fixed $\rho = 0.001$. The thick line is the theoretical prediction.

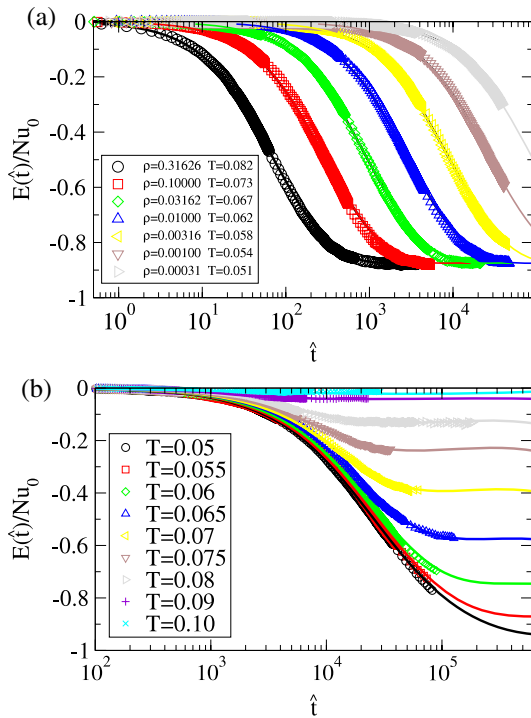


Figure 7. Evolution of the potential energy per particle (symbols) and theoretical predictions (lines) for all studied simulations. In (a), simulations refer to different ρ and T values, such that the final equilibrium state is characterized by $\bar{l} = 8$. In (b), $\rho = 0.001$.

dependence of the energy is well described by the analytic theory.

5.3. Extent of polymerization

Experimentalists often consider a quantity called *progress curves* in their characterization of the self-assembly of polymer chains. This is defined as the time dependent extent of polymerization $\Phi(t)$, which is normally measured spectroscopically. $\Phi(t)$ is defined as the fraction of particles

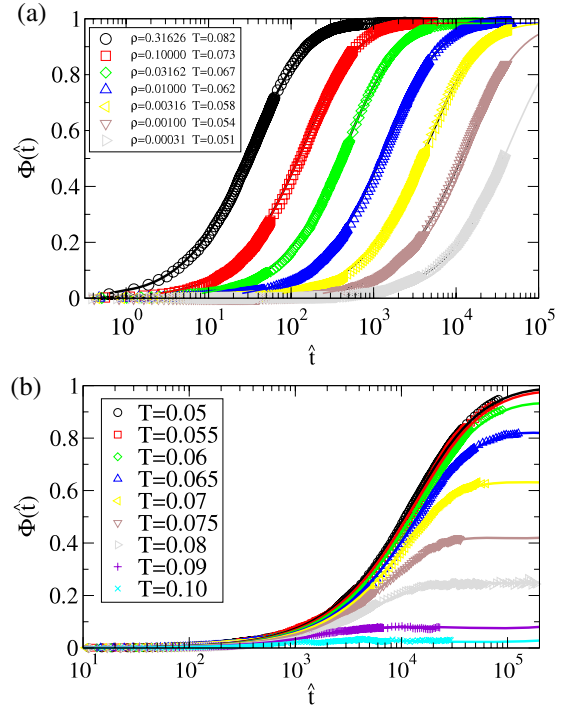


Figure 8. Time dependence of the extent of reaction for the studied model for (a) simulations with different ρ and T values, such that the final equilibrium state is characterized by $\bar{l} = 8$ and (b) for simulation at fixed $\rho = 0.001$. The thick lines are the theoretical prediction. Note that the polymerization transition temperature for the $\rho = 0.001$ case is $T = 0.072$.

connected in chains (chain length larger than one), i.e.,

$$\Phi(t) = \frac{\sum_{l=2}^{\infty} l N_l(t)}{\sum_{l=1}^{\infty} l N_l(t)} = 1 - \frac{N_1(t)}{N} = 1 - \bar{l}(t)^{-2} \quad (23)$$

where we have used equation (18). Φ plays the role of order parameter for the polymerization transition. Since $\frac{1}{\sqrt{1-\Phi(t)}} = \bar{l}(t)$, the time dependence of $\Phi(t)$ is analytically determined by equation (20),

$$\Phi(t) = 1 - \left[\frac{2}{1 + (2\bar{l} - 1) \tanh\left[\frac{k_{\text{breaking}} t}{2} (2\bar{l} - 1) - \phi\right]} \right]^2. \quad (24)$$

Despite the time dependence of the extent of reaction is simply a transformation of the time dependence of $\bar{l}(t)$, it is instructive to show (in figure 8) the behavior of the numerical curves for Φ and compare them with equation (24), for the two set of simulations. The curves approach a constant value at large times, coincident with $1 - \bar{l}^{-2}$. In the set of simulations where $\bar{l} = 8$, the curves are identical and can be collapsed by scaling the time by k_{breaking}^{-1} .

An universal representation of the progress curve (identical to the one of $\bar{l}(t)$) for chain polymerization can be obtained from the previous expression by noting that

$$\frac{\frac{2}{\sqrt{1-\Phi(t)}} - 1}{\frac{2}{\sqrt{1-\Phi}} - 1} = \tanh\left[\frac{k_{\text{breaking}} t}{2} (2\bar{l} - 1) - \phi\right], \quad (25)$$

where we have defined $\bar{\Phi}$ as the equilibrium polymerization (infinite time value of $\Phi(t)$). An experimental representation of the extent of polymerization in this form versus time should show the typical tanh shape. As for the case of $\bar{l}(t)$, for large \bar{l} , $\phi \rightarrow 0$ and curves for different systems collapse on the same universal curve if time is scaled by $[k_{\text{breaking}}\bar{l}]^{-1}$.

6. Conclusions

This paper describes a numerical study of the dynamic theory of equilibrium polymer in the absence of constraints on the polymerization process (e.g., chemical and thermal activation), expanding on pioneering MC studies by Milchev and Rouault [50–52]. We perform Brownian dynamics simulations, to generate a realistic dynamics of the chains in solution and to be able to compare the dimer association rate constant with theoretical predictions. The choice of a simple model which can be solved analytically within the Wertheim theory makes it possible to provide an almost full description of the equilibration dynamics without introducing any fit parameter. Indeed, the entire evolution of the system can be predicted based on knowledge of the monomer density, the temperature and the dimer Brownian association constant k_{bonding} . This quantity can in principle be evaluated independently (being a property of the model) and it would be informative to evaluate the dependence of the association constant on the number and geometry of the particle patches [65, 67], a topic also relevant for protein–protein association [68–70].

We focus on the time evolution of the average chain length and two related quantities, the potential energy and the equilibrium polymerization order parameter $\Phi(t)$ (or progress curve) governing self-assembly growth, following a T -jump. We find that the rate of polymerization ordering following a jump from the disordered to ordered thermodynamic by lowering the temperature involves two competing factors, a factor related to the solution viscosity (via the modulation of the bonding constant k_{bonding}) and thermodynamic factor that progressively increases as the temperature is lowered below the polymerization transition (via \bar{l}). This trend is typical of many order–disorder transitions

According to the Smoluchowski equations describing the evolution of the system after a T -jump (equation (2)), the equilibration process proceeds via a sequence of transient configurations, each of them characterized by an exponential chain length distribution, allowing for a precise association of the equilibration time with a fictive temperature. Equilibrium polymerization could be thus considered as a model system for testing recent theoretical developments on the violation of the fluctuation-dissipation theorem [71] in aging systems. The potential energy landscape [72] is particularly simple for this model, which should aid in comprehending the aging phenomenon. It also suggests that chemical step polymerization for bifunctional compounds, which could be considered as a $t \rightarrow 0$ quench, also proceeds via a sequence of exponential distribution of chain lengths. It would be particularly interesting to explore if the evolution of the system proceeds via a sequence of equilibrium configurations also in the case of multifunctional assembling particles, at least

in the limit in which loops are missing [41]. We also note that for the case of living polymerization (which is distinct from the equilibrium polymerization case discussed here) it has been suggested [66] that the evolution of the chain length distribution following a temperature jump is characterized by an evolving non-exponential distribution of chain lengths. The ‘living’ polymers apparently preferentially ‘eat their young’, resulting in a long-lived peak in the mass distribution.

Our study provides a framework for estimating the rate of self-assembling ordering, in real assembling systems exhibiting equilibrium polymerization in terms of molecular parameters. Of course, independent estimates of the bonding free energy (equation (10)) are required also for such estimates of self-assembly dynamics. One major difficulty is the assumption of treating the background solvent as a continuum fluid devoid of atomic characteristics. In general the solvent, and even small concentrations of additives, especially polymer species will modify the enthalpic and entropic parameters governing self-assembly. Experimental studies seem to indicate that the changes in the entropy and enthalpy of assembly tend to be correlated (enthalpy–entropy compensation [73–75]) and a general study of such effects could be profitable. Up to now, there is no way to predict the fundamental equilibrium association constants governing self-assembly from molecular information. This difficulty is especially severe in the case of aqueous solutions of associating species since water itself is a complex associating fluid. It is then crucial to begin studying how self-assembly becomes modified when the solvent itself is an associating fluid. This is a complicated problem, but one which can be attacked by MD and MC simulation methods. We expect that the framework that we have developed in this paper will be useful for interpreting simulations of this kind and a starting point of for the development of physically more realistic analytic theories that take into account effects on self-assembly that arise from this process occurring in a condensed liquid state in the presence of molecules distinct from the assembling particles of interest.

There are other challenges to treating assembly in fluids beyond the renormalization of the energetic parameters governing assembly and which are missing in our model. We need to consider the presence of inter and intramolecular hydrodynamic interactions between the chain segments that can dramatically alter the rate of chain diffusion and the nature of stress relaxation in such fluids. This type of problem is simply not tractable from an analytic standpoint, but there are powerful simulation methods such lattice Boltzmann [76] and dissipative particle dynamics [77] methods that can address this difficult problem. We mention the promising work of Dünweg and co-workers on the origin of hydrodynamic screening in polymer (static rather than dynamic) solutions [78] as a good example of the possibilities of this approach. Finally, we must also acknowledge the importance of topological (entanglement) interactions between the chains that restrict their crossing in the limit of long chains.

In short term, it is important to establish how multifunctionality of particle association influences the nature of the particle self-assembly. Glotzer [10, 79] and

van Workum and Douglas [13] have both found evidence that self-assembly transition can become appreciably sharper (thermodynamically) when the associative interactions become multifunctional instead of bifunctional as in the present study. Indeed, Glotzer and co-workers have argued that there is a general tendency for the self-assembly transition to become a first order phase transition. Van Workum [13] simply noted that such transitions became significantly sharper with variation in temperature and were thus harder to simulate at equilibrium. If the transition is indeed first order, then it will be necessary to model nucleation processes governing the emergence of new phases in this type of self-assembly. Initiation of growth in these systems normally involves structures that are spherical droplet-like structures so that a reformulation of classical nucleation theory would be required to describe growth initiation in systems exhibiting polymerization with multifunctional interactions [13]. Clearly, there are many challenges ahead in modeling the thermodynamics and dynamics of even the simplest self-assembling systems.

Acknowledgments

We acknowledge support from MIUR-Prin and MCRTN-CT-2003-504712.

Appendix

Our Brownian dynamics algorithm is an extension of the algorithm recently developed for particles interacting with hard-sphere and the square-well potentials [80] and adopted in the recent studies of Brownian dynamic studies of interacting colloids [81, 82]. The extension to non-spherical particles of mass m requires a description of the rotational motion of the particles. Assuming that the three moments of inertia, along the principal axes of each particle, are all equal, i.e. $I_x = I_y = I_z = I$ and defining \vec{v}_i and $\vec{\omega}_i$ as the center-of-mass velocity and the angular velocity of particle i respectively, the algorithm is based on the iteration of the following steps:

- (i) For every $t_n = n\delta t$, with n integer number, for all particles ($i = 1 \dots N$, where N is the total number of particles) we specify the center-of-mass velocities $\vec{v}_i \equiv (v_{x,i}, v_{y,i}, v_{z,i})$ according to a Maxwellian distribution $P_t(\vec{v}_i)$:

$$P_t(\vec{v}_i) = \left(\frac{m}{2\pi T}\right)^{3/2} e^{-m \frac{v_{x,i}^2 + v_{y,i}^2 + v_{z,i}^2}{2T}} \quad (26)$$

and then specify angular velocities $\vec{\omega}_i \equiv (\omega_{x,i}, \omega_{y,i}, \omega_{z,i})$ according to the distribution $P_r(\vec{\omega}_i)$, defined as follows:

$$P_r(\vec{\omega}_i) = \left(\frac{I}{2\pi T}\right)^{3/2} e^{-I \frac{\omega_{x,i}^2 + \omega_{y,i}^2 + \omega_{z,i}^2}{2T}}. \quad (27)$$

In addition the component of the angular velocity along the direction, we join the centers of the two sticky spots of each particle, is set to 0, due to the symmetry of the particles around such an axis.

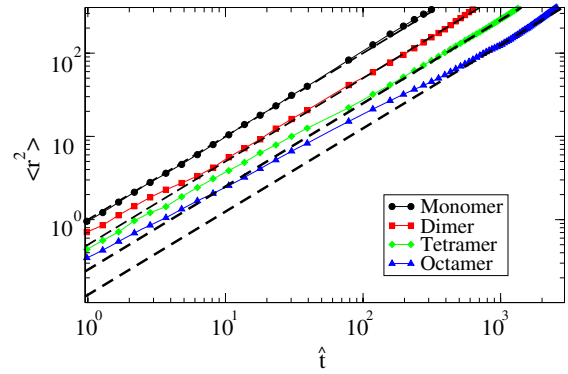


Figure 9. Mean square displacement of a monomer belonging to polymers of length one, two, four and eighth. Dashed curves are the expected theoretical values for the long time diffusion, $\langle \hat{r}^2 \rangle = 6D_M \hat{t}$, where $D_M = D_1/M$.

- (ii) We then evolve the system between t_n and $t_n + \delta t$ according to the laws of ballistic motion of rigid bodies with mass m and moment of inertia I (performing event driven molecular dynamics).

The time δt is related to the monomer translational diffusion constant D_1 by the relation $D_1 = \frac{k_B T \delta t}{2m}$. The corresponding rotational diffusion coefficient is $D_R = \frac{k_B T \delta t}{2I}$. We have used the sphere inertia moment $I = \frac{m\sigma^2}{10}$ and $\delta t = 0.5$ (in units of $\sqrt{m\sigma^2/u_0}$).

To check that the Brownian dynamics code reproduces a realistic dynamics, we performed a set of ‘control’ simulations of isolated chains having length 1 (monomer), 2 (dimer), 4 (tetramer) and 8 (octamer)—at a very small T so that no bond breaking events are observed during the simulation time. Figure 9 shown the mean square displacement of an arbitrary monomer belonging to clusters of different size. At long time, where rotational processes are averaged out, the slope of the mean square displacement versus time approaches the diffusion coefficient of the chain center of mass. It is seen that the algorithm correctly generates a diffusion process which scales with the inverse of the size (mass) of the chains, i.e. Rouse dynamics. Hence the center of mass diffusion D_M of a cluster of size M scales as D_1/M .

References

- [1] Manoharan V N, Elsesser M T and Pine D J 2003 *Science* **301** 483
- [2] Mirkin C A, Letsinger R L, Mucic R C and Storhoff J J 1996 *Nature* **382** 607
- [3] Cho Y-S, Yi G-R, Lim J-M, Kim S-H, Manoharan V N, Pine D J and Yang S-M 2005 *J. Am. Chem. Soc.* **127** 15968
- [4] Yi G, Manoharan V N, Michel E, Elsesser M T, Yang S and Pine D J 2004 *Adv. Mater.* **16** 1204
- [5] Cho Y-S, Yi G-R, Kim S-H, Pine D J and Yang S-M 2005 *Chem. Mater.* **17** 5006
- [6] Mirkin C, Letsinger R, Mucic R and Storhoff J 1996 *Nature* **382** 607
- [7] Starr F W, Douglas J F and Glotzer S C 2003 *J. Chem. Phys.* **119** 1777
- [8] Glotzer S C 2004 *Science* **306** 419

- [9] Glotzer S C, Solomon M J and Kotov N A 2004 *AICChE J.* **50** 2978
- [10] Zhang Z and Glotzer S C 2004 *Nano Lett.* **4** 1407
- [11] Doye J P K, Louis A A, Lin I-C, Allen L R, Noya E G, Wilber A W, Kok H C and Lyus R 2007 Controlling crystallization and its absence: proteins, colloids and patchy models <http://www.citebase.org/abstract?id=oai:arxiv.org:cond-mat/07%01074>
- [12] Starr F W and Sciortino F 2006 *J. Phys.: Condens. Matter* **18** L347 (Preprint cond-mat/0512260)
- [13] Van Workum K and Douglas J F 2006 *Phys. Rev. E* **73** 031502
- [14] Stupp S I, Son S, Lin H C and Li L S 1993 *Science* **259** 59
- [15] Mirkin C A 2000 *Inorg. Chem.* **39** 2258
- [16] Douglas T and Young M 1998 *Nature* **393** 152
- [17] Pattenden L K, Middelberg A P J, Niebert M and Lipin D I 2005 *Trends Biotechnol.* **23** 523
- [18] Rothemund P W K 2006 *Nature* **440** 297
- [19] Liepold L O, Revis J, Allen M, Oltrogge L, Young M and Douglas T 2005 *Phys. Biol.* **2** S166
- [20] Douglas T and Young M 2006 *Science* **312** 873
- [21] Xu L, Frederik P, Pirollo K F, Tang W-H, Rait A, Xiang L-M, Huang W, Cruz I, Yin Y and Chang E H 2002 *Hum. Gene Ther.* **469-481** 13
- [22] Strable E, Johnson J E and Finn M G 2004 *Nano Lett.* **4** 1385
- [23] Wang Q, Lin T, Tang L, Johnson J E and Finn M G 2002 *Angew. Chem. Int. Edn* **41** 459
- [24] Mao C, Solis D J, Reiss B D, Kottmann S T, Sweeney R Y, Hayhurst A, Georgiou G, Iverson B and Belcher A M 2006 *Science* **303** 213
- [25] Lee S-W, Mao C, Flynn C E and Belcher A M 2002 *Science* **296** 892
- [26] Douglas T, Strable E, Willits D, Aitouchen A, Libera M and Young M 2002 *Adv. Mater.* **14** 415
- [27] Largo J, Starr F W and Sciortino F 2007 *Langmuir* **23** 5896
- [28] Stambaugh J, Workum K V, Douglas J F and Losert W 2005 *Phys. Rev. E* **72** 031301
- [29] Tang Z, Zhang Z, Wang Y, Glotzer S C and Kotov N A 2006 *Science* **314** 274
- [30] Klokkenburg M, Houtepen A J, Koole R, de Folter a B H E J W J, van Faassen E and Vanmaekelbergh D 2007 *Nano Lett.* **7** 2931
- [31] Van Workum K and Douglas J F 2005 *Phys. Rev. E* **71** 031502
- [32] Rapaport D C 2004 *Phys. Rev. E* **70** 051905
- [33] Douglas J F and van Workum K 2007 *J. Mater. Res.* **22** 24
- [34] Glotzer S C and Solomon M J 2007 *Nat. Mater.* **6** 557
- [35] Fejer S N and Wales D J 2007 *Phys. Rev. Lett.* **99** 086106
- [36] Dudowicz J, Freed K F and Douglas J F 1999 *J. Chem. Phys.* **111** 7116
- [37] Dudowicz J, Freed K F and Douglas J F 2003 *J. Chem. Phys.* **119** 12645
- [38] Douglas J F, Dudowicz J and Freed K F 2006 *J. Chem. Phys.* **125** 4907
- [39] Dudowicz J, Freed K F and Douglas J F 2000 *J. Chem. Phys.* **113** 434
- [40] Zlotnik A 1994 *J. Mol. Biol.* **241** 59
- [41] Bianchi E, Tartaglia P, La Nave E and Sciortino F 2007 *J. Phys. Chem. B* **111** 11765
- [42] Wertheim M 1984 *J. Stat. Phys.* **35** 19
- [43] Wertheim M 1984 *J. Stat. Phys.* **35** 35
- [44] Wertheim M 1986 *J. Stat. Phys.* **42** 459
- [45] Sciortino F, Bianchi E, Douglas J F and Tartaglia P 2007 *J. Chem. Phys.* **126** 4903
- [46] Dudowicz J, Freed K F and Douglas J F 2004 *Phys. Rev. Lett.* **92** 045502
- [47] Bianchi E, Largo J, Tartaglia P, Zaccarelli E and Sciortino F 2006 *Phys. Rev. Lett.* **97** 168301
- [48] Marques C M and Cates M E 1991 *J. Physique II* **1** 489
- [49] Cates M E and Candau S J 1990 *J. Phys.: Condens. Matter* **2** 6869
- [50] Milchev A and Rouault Y 1995 *J. Physique II* **5** 343
- [51] Rouault Y and Milchev A 1996 *Europhys. Lett.* **33** 341
- [52] Rouault Y and Milchev J 1995 *Phys. Rev. E* **51** 5905
- [53] Huang C-C, Xu H and Ryckaert J-P 2006 *J. Chem. Phys.* **125** 4901
- [54] Douglas J F, Efimenko K, Fischer D A, Phelan F R and Genzer J 2007 *Proc. Natl Acad. Sci.* **104** 10324
- [55] Ferrone F A, Hofrichter J, Sunshine H R and Eaton W A 1980 *Biophys. J.* **32** 361
- [56] Scott R L 1965 *J. Chem. Phys.* **69** 261
- [57] Wheeler J C, Kennedy S J and Pfeuty P 1980 *Phys. Rev. Lett.* **45** 1748
- [58] Greer S C 1988 *J. Phys. Chem. B* **102** 5413
- [59] Greer S C 1996 *Adv. Chem. Phys.* **94** 261
- [60] Greer S C 2002 *Annu. Rev. Phys. Chem.* **53** 173
- [61] Hinz H and Sturtevant J M 1972 *J. Biol. Chem.* **247** 3697
- [62] Russel W B, Saville D A and Schowalte W R 1991 *Colloidal Dispersions* (Cambridge: Cambridge University Press)
- [63] Stukalin E B and Freed K F 2006 *J. Chem. Phys.* **125** 4905
- [64] Oshanin G and Moreau M 1995 *J. Chem. Phys.* **102** 2977
- [65] Schlosshauer M and Baker D 2002 *J. Phys. Chem. B* **106** 12079
- [66] O'Shaughnessy B and Vavylonis D 2003 *Phys. Rev. Lett.* **90** 1180301
- [67] Moncho-Jordá A, Odriozola G, Tirado-Miranda M, Schmitt A and Hidalgo-Álvarez R 2003 *Phys. Rev. E* **68** 011404
- [68] Gabboulline R R and Wade C 2001 *J. Mol. Biol.* **306** 1139
- [69] Northrup S H and Erickson H P 1992 *Proc. Natl Acad. Sci. USA* **89** 3338
- [70] Schlosshauer M and Baker D 2004 *Protein Sci.* **13** 1660
- [71] Sciortino F and Tartaglia P 2001 *Phys. Rev. Lett.* **86** 107
- [72] Sciortino F 2005 *J. Stat. Mech.: Theory Exp.* **5** 15
- [73] Bedö Z, Bercz E and Lakatos I 1992 *Colloid Polym. Sci.* **270** 799
- [74] Chen L-J, Lin S-Y and Huang C-C 1998 *J. Phys. Chem. B* **102** 4350
- [75] Liu L and Guo Q-X 2001 *Chem. Rev.* **101** 673
- [76] Cates M E, Stratford K, Adhikari R, Stansell P, Desplat J-C, Pagonabarraga I and Wagner A J 2004 *J. Phys.: Condens. Matter* **16** 3903
- [77] Soddemann T, Dünweg B and Kremer K 2003 *Phys. Rev. E* **68** 046702
- [78] Ahlrichs P, Everaers R and Dünweg B 2001 *Phys. Rev. E* **64** 040501
- [79] Zhang Z, Horsch M A, Lamm M H and Glotzer S C 2003 *Nano Lett.* **3** 1341
- [80] Scala A, Voigtmann T and De Michele C 2007 *J. Chem. Phys.* **126** 4109
- [81] Foffi G, De Michele C, Sciortino F and Tartaglia P 2005 *Phys. Rev. Lett.* **94** 078301
- [82] Foffi G, De Michele C, Sciortino F and Tartaglia P 2005 *J. Chem. Phys.* **122** 4903